Flexural Characteristics of RC Beams Made of Graphite Tailings in a Chloride Environment

[1*] *Ms. Edara Krishna Reddy,* [2]*Ms. Puja Priyadarshini Sahoo*
[1*]*Asso. Professor, Dept. OF Civil Engineering, NIT BBSR,*
Asst. Professor DEPT. of Civil Engineering, INDIC, BBSR
[1*]*rdarakrishna@thenalanda.com , sahoopuja@gmail.com*

ABSTRACT: This study examines the mechanical characteristics of concrete beams made from graphite tailings under various curing settings. The findings demonstrate that the mechanical properties of concrete are significantly influenced by the concentration of graphite tailings. The improved bearing capacity calculation formula and the beam's bending properties are obtained in the end, providing a theoretical foundation and a benchmark for the development of green building materials. The primary innovations and key discoveries of this paper's research are as follows: (1) The fracture load and ultimate load of concrete beams with a 20% replacement rate for graphite tailings are the highest in the three types of concrete trial environments. (2) In the three different concrete test environments, when the test beams were subjected to the same load and the replacement rate of the graphite tailings increased, the mid-span deflection of the concrete beams exhibited a trend of first reducing and then increasing. The test beam's mid-span deflection is lowest at a replacement rate of 20% for graphite tailings sand. (3) By experiments, it is discovered that the plane section assumption holds true for the normal section bearing capacity of concrete beams made from graphite tailings following chloride salt erosion. After chloride salt erosion, the longitudinal tensile steel bar of concrete beams with various rates of replacing the sand with graphite tailings experiences the same strain as standard concrete beams, and the slope of the strain curve exhibits the same linear trend. The experimental findings indicate that the strain on steel bars is not significantly affected by the pace at which graphite tailings sand is replaced. (4) The experimental value of a concrete beam's normal section bearing capacity is fitted using the Gauss function, and a calculation formula for the normal section ultimate bearing capacity of a concrete beam made of graphite tailings sand in a chloride environment is established. The examination of the mechanical properties of graphite tailings sand and concrete components can greatly benefit from the research findings presented in this work as a reference.

1. Introduction

With the growth of the Chinese economy in recent years, coastal city construction has accelerated [1]. A lot of concrete is required for large-scale infrastructure construction, which depletes natural stone resources and has detrimental environmental effects [2–5]. Alternative raw materials must be discovered in order to effectively limit the use of natural stone. Years of study have revealed that graphite tailings sand can be utilised in place of natural sand [6, 7]. In addition to significantly reducing the need for natural sand, a sensible use of graphite tailings sand can also eliminate environmental damage [8–10]. Due to their service environment, coastal structures are susceptible to salt-ion erosion, which affects their durability concrete structural failure [11–13]. Whenever the structures are harmed, there will unavoidably be significant financial losses. Studying the mechanical characteristics of concrete structures in coastal environments is vital to prevent the breakdown of concrete buildings.

The breakdown of concrete structures is caused by a variety of circumstances. Among these, chloride ion erosion is the primary reason for steel corrosion, which directly causes concrete structures to lose their durability [14, 15]. Steel corrosion occurs as a result of the destruction of the steel passivation coating caused by chloride ions penetrating the concrete [16, 17]. Under conditions of chloride erosion, Shang-Qin [18] tested concrete beams for bending. The test findings demonstrate that as service time grows, concrete beams' ultimate bearing capacity initially rises and then falls.

At the same time, based on the test results and the existing specifications, the formula for calculating the bearing capacity of concrete beams suitable for marine environment is obtained. Yin et al. [19] also conducted similar tests. The test results show that with the increase of the number of dry and wet cycles, the crack width and mid-span deflection of the test beam gradually increases, and the ultimate bearing capacity of the test beam gradually decreases.

Chloride corrosion is the main cause of steel corrosion, and steel corrosion is the first factor afecting the durability of concrete structures [20–22]. Chloride penetrates concrete, destroys steel passive film, and causes steel corrosion [23–25]. In recent years, Hong-Bo et al. [26–30] studied the influence of graphite tailings on the properties of cement-based materials and concrete blocks. The results show that the mechanical properties of cement-based materials can be improved by adding an appropriate amount of graphite tailings. Compared with ordinary concrete, low-content of graphite tailings concrete has better compressive strength, compressive sensitivity, and impermeability. Sun [31] studied the influence of graphite tailings incorporation ratio on the mechanical properties of foamed concrete, and the results show that the appropriate amount of graphite tailings incorporation can improve its compressive strength.

In summary, the research on the durability of graphite tailings concrete focuses on the permeability and resistance to chloride ion erosion of concrete test blocks under chloride salt erosion, while the mechanical properties of graphite tailings concrete components in a chloride salt environment such as bending resistance are less studied. The authors of this paper and their research team have conducted research on related issues and have achieved certain results [32]. To better improve the research paper, in this paper, the bending test of graphite tailings concrete beams with diferent substitution rates under three curing environments of air, water, and chloride salt is conducted. The failure mode, crack propagation law, load characteristic value, mid-span deflection, and strain of the concrete and steel bar of the test beams under three curing environments are analyzed. According to the above experimental values, a new calculation formula has been established. The above research results will provide good guidance value for similar research on graphite tailings concrete members.

2. Test Overview

Materials and Mixtures Ratio

(1) Cement: P.O42.5 ordinary Portland cement.

(2) Stone: particle size of 5∼20 mm, good gradation, apparent density of 2650 kg/m^3.

(3) Natural river sand: river sand with a fineness modulus of 2.49.

(4) Graphite tailings: graphite tailings from the graphite tailings reservoir.

(5) Poly carboxylic water reducer: MZ-10C poly-carboxylic high performance water reducer is selected from Table 1.

(6) Steel bar: HRB400 bar is used. And its diameter is 10 mm, and its yield strength is 415 MPa.

The physical characteristics of natural sand and graphite tailings is shown in Table 1.

Proportion Relation of Concrete Component Materials. According to the mix proportion in Table 2, graphite tailings concrete beams with substitution rates of 0, 10%, 20%, 30%, and 40% were prepared. It should be noted that the sand ratio in the table is 30%, which is significantly lower than that of the common pumping concrete in the project. This is because the fineness modulus of sand is small, and there are many particles in the sand, and the cohesion of the concrete is easy to be guaranteed. Therefore, small sand ratio is adopted, and this test is nonpumping concrete. The sand ratio of pumping concrete is 2%–5% higher than that of nonpumping concrete, so the sand ratio used in this test is lower than that of pumping concrete in the project.

Experimental Design. In this experiment, three groups of graphite tailings concrete beams (air, fresh water, and chloride environment, respectively, expressed by SMK, FE, and CE) were designed, and five concrete beams were made in each group. One of the beams was a natural sand concrete beam as the contrast beam, and the four roots were graphite tailings concrete beams, with substitution rates of 10%, 20%, 30% and 40%, respectively. The number of graphite tailings concrete beams in chloride environment was CE-0, CE-10, CE-20, CE-30, and CE-40. The number of graphite tailings concrete beams in air and freshwater environment was the same. The test beam size is length 1600 mm, section size is 120 mm×180 mm, and net span is 1500 mm. To study the flexural performance of graphite tailings concrete beams in three environments, all test beams adopt the same reinforcement ratio. The reinforcement ratio of longitudinal tensile reinforcement is 1.257%, and the thickness of the longitudinal reinforcement protective layer is 20 mm. Specimen production and environmental erosion processes are shown in Figure 1. The size and reinforcement of the beam are shown in Figure 2. Each reinforced concrete beam was made, and three cube test blocks were prepared at the same time. After the same condition of maintenance, the same environmental corrosion was conducted with the same group of test beams.

Test Scheme and Measurement Content. Chlorine salt erosion test using 10% NaCl solution, natural immersion 120 d. The loading test adopts a three-point loading mode, forming a 500 mm pure bending section in the middle of the span. The loading device and the layout of the measuring points are shown in Figure 3. According to the standard of concrete structure test method, the bending test of concrete beams after environmental action is conducted [33]. The concentrated load is applied by a hydraulic press, and the pressure sensor is placed in the span of the distribution beam to realize the loading mode of two concentrated forces and three points. Before the test loading, the test beam is

Table 1: Physical properties of graphite tailings sand and natural sand.

Physical property	Grain size (mm)	Apparent density ($kg \cdot m^{-3}$)	Bulk density ($kg \cdot m^{-3}$)	Fineness modulus	Water absorption (%)	pH value
Natural sand	0.16~5	2620	1540	2.49	21.87	8
Graphite tailings	0.01~3	2855	1630	0.90	30.10	10

Table 2: Mix ratio and mechanical properties of 1 m^3 graphite tailing sand concrete.

Test specimen number	Volume of concrete materials (kg/m^3)						Water cement ratio	Percentage of sand (%)
	Water	Cement	Natural sand	Pebble	Graphite tailings	Water reducing admixture		
SMK-0	180.00	409.09	535.48	1294.45	0	15.68	0.44	30
SMK-10	180.00	409.09	481.93	1294.45	53.55	15.68	0.44	30
SMK-20	180.00	409.09	428.38	1294.45	107.10	15.68	0.44	30
SMK-30	180.00	409.09	374.84	1294.45	160.64	15.68	0.44	30
SMK-40	180.00	409.09	321.29	1294.45	214.19	15.68	0.44	30

Note. Specimen number SMK-*n*, SMK represents test beam, *n* represents graphite tailings replacement rate value. For example, SMK-20 represents the test beam with graphite tailings replacement rate of 20%. Among them, SMK-0 is the ordinary concrete control beam.

(a) (b)

Figure 1: Specimen production and environmental erosion process. (a) The specimen-making process. (b) Environmental erosion process.

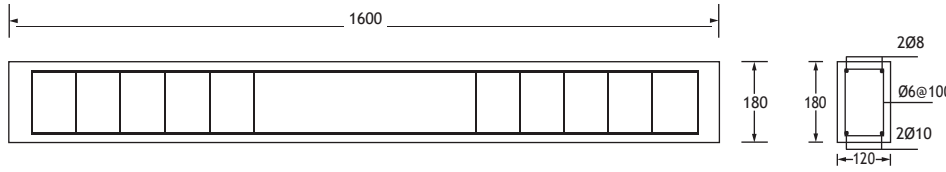

Figure 2: Size and reinforcement diagram of the test beam (unit: mm).

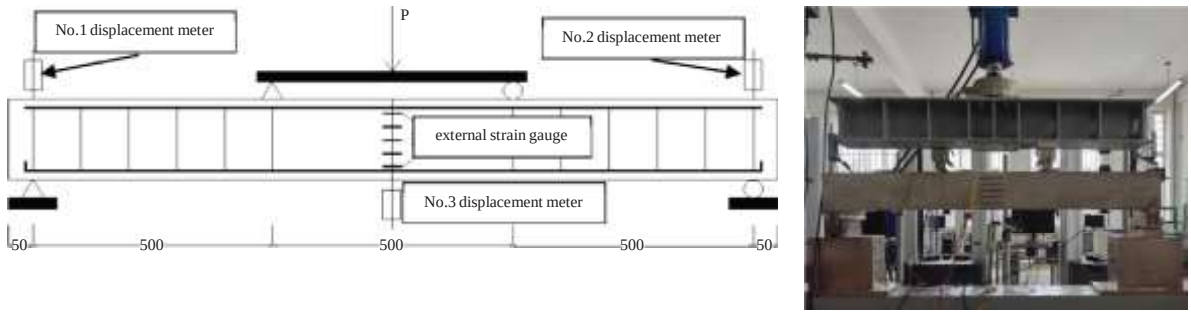

(a) (b)

Figure 3: Layout of measuring points and loading device diagram. (a) Layout of measuring points. (b) Loading device.

preloaded to ensure the normal operation of the instrument and the normal contact of each point. At the beginning, the loading mode was according to each level of 3 kN loading, each loading stayed for 3 minutes, and then the change of cracks on the surface of the beam was observed, when the specimen's first crack appeared, with each level of 5 kN for diferential loading and gradual increase of load, the number of cracks gradually increased, cracks continued to extend upward and the crack width increased, with the pen to thicken the cracks of the test beam, in order to more clearly see the cracks of the test beam, and record the stress load and crack width.

The main measurement contents of the test are as follows: (1) Cracking load, ultimate load and crack development process of the test beam, and the crack development process is observed by the DJCK-2 crack width meter. (2) The strain of reinforcement and concrete is measured by sticking strain gauges in the middle of the tensile reinforcement, and five concrete strain gauges are evenly arranged along the height of the beam in the middle of the beam span to measure the strain of concrete; (3) Load-deflection changes, YHD-50 displacement gauges arranged at both ends of the beam and the middle of the beam to measure the deformation of the specimen.

3. Experiment Results and Analyses

Crack Propagation Distribution Law. Through the bending load test of the test beam, it is found that the failure process and crack development process of the graphite tailings concrete beam in the three environments are consistent with those of the ordinary concrete beam. The failure mode and crack development process of each test beam in the fresh water and chloride environments are also basically consistent with those in the air environment, but the characteristic load changes slightly. The bending failure mode and crack distribution of the test beam in the fresh water and chloride environment, are shown in Figure 4.

Cracking Load and Ultimate Load of Beam. The test results of the cracking load P_{cr} and ultimate load P_u of each test beam under air, water and chloride environment are shown in Table 3. The efects of diferent variation parameters on cracking load and ultimate load of test beam are shown in Figures 5 and 6. It can be seen from Table 3 and Figures 5 and 6.

Efects of Diferent Graphite Tailings Replacement Ratios on Cracking Load and Ultimate Load of Test Beams. It can be seen from Table 3 and Figure 5 that with the increase of graphite tailings replacement rate, the variation laws of cracking load and ultimate load of test beams in air, water, and chlorine salt are the same, showing a trend of first increase and then decrease. Among them, in the chloride environment, the cracking loads of CE-10 and CE-20 in- creased by 12.64% and 15.97%, respectively, compared with CE-0, and the ultimate load increased by 6.78% and 8.93%, respectively. The cracking load and ultimate load of CE-40 decreased by 8.39% and 5.00% compared with CE-0. The results show that with the increase of graphite tailings replacement rate, the performance of test beams in diferent environments is better than that of ordinary concrete beams at the replacement rate of 10%∼20%, and the bearing capacity is lower than that of ordinary concrete beams at the replacement rate of 40%. The reason is that when the replacement rate of graphite tailings is 10%∼20%, the diameter of graphite tailings is smaller than that of natural sand, which makes the distribution of particles in concrete more uniform, increases the compactness of concrete materials and improves the bearing capacity of graphite tailings concrete beams.

Influence of Diferent Erosion Environment on Cracking Load and Ultimate Load of Graphite Tailings Concrete Beam. It can be seen from Table 3 and Figure 6 that the bearing capacity of the test beam under a clear water environment is the highest under the same replacement rate of graphite tailings, and the bending bearing capacity of the test beam after chlorine salt erosion is lower than that in an air (noncorrosion) environment. Taking the replacement rate of graphite tailings 20%, as an example, the cracking load and ultimate load of graphite tailings concrete beams in a clear water environment are increased by 6.74% and 4.87%, respectively, compared with those in an air environment. This is because the hydration reaction can continue to occur in the test beam in a clear water environment, and the hy- dration products are generated to make the concrete denser, thus enhancing the bearing capacity of the test beam. However, the cracking load and ultimate load of graphite tailings concrete beams after chloride corrosion are 3.82% and 2.03% lower than those in an air environment, re-spectively. It is also found that the cracking load is more afected by environmental erosion than the ultimate load, indicating that the bearing capacity of reinforced concrete beams immersed in a 10% NaCl solution for 120 days is more afected by concrete damage.

Mid-Span Deflection. The load-deflection curves of concrete beams with diferent graphite tailings replacement rates in air, water, and chloride environments are shown in Figures 7(a)–7(c). To compare the change law of mid-span deflection of concrete beams with the same graphite tailings replacement rate after erosion in diferent environments with load, the load-deflection curves of concrete beams with a 20% graphite tailings replacement rate after erosion in air, water, and chloride environments are plotted, as shown in Figure 7(d). From Figure 7, it can be seen that the load-deflection curve trend of a graphite tailings concrete beam and an ordinary concrete beam is similar, which can be divided into three stages: (1) The noncracking stage of the test beam: at the initial stage of loading, the test beam is not cracked, the load-deflection curve is approximately linear change, and the deflection increment is small. (2) The test beam cracked at the yield stage of reinforcement. After the test beam cracked, the load-deflection curve showed a turning point, and the growth rate of deflection gradually accelerated.

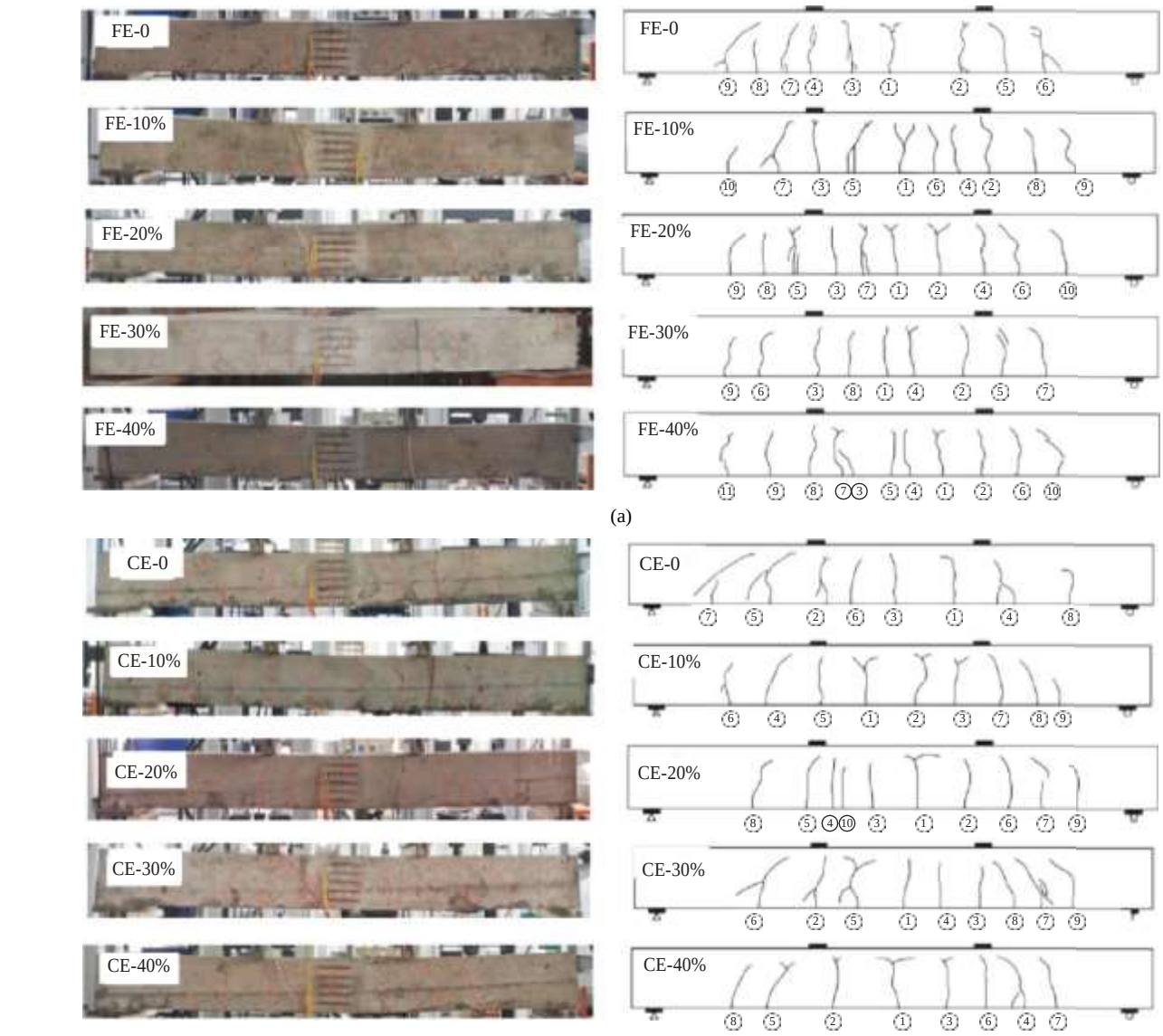

Figure 4: Bending failure mode and crack distribution map of test beam under water and chloride environment. (a) Fresh water environment and (b) chloride environment.

Table 3: Test values of cracking load and ultimate load of test beams in three environments.

Graphite tailings sand replacement rate (%)	Air environment		Clear water environment		Chlorine environment	
	P_{cr} (kN)	P_u (kN)	P_{cr} (kN)	P_u (kN)	P_{cr} (kN)	P_u (kN)
0	12.12	49.25	12.42	50.85	11.08	47.81
10	13.25	52.01	13.37	53.17	12.48	51.05
20	13.36	53.16	14.26	55.75	12.85	52.08
30	12.43	50.33	13.17	52.42	11.51	49.26
40	11.21	47.01	12.12	49.17	10.15	45.42

The load-deflection curve gradually developed nonlinearly after cracking. (3) The steel bar yield to the failure stage: after the steel bar yield, the load-deflection curve appears the second turning point, and the deflection of the beam increases sharply after yield. The load-deflection curve is also close to a horizontal straight line, and the final test beam is damaged.

Specifically, it can be seen from Figures 7(a) and 7(b) that when the test beam bears the same level of load in an air and clear water environment, with the increase of the graphite tailings replacement rate, the mid-span deflection of the test beam decreases first and then increases. When the replacement rate is 20%, the mid-span deflection of the test

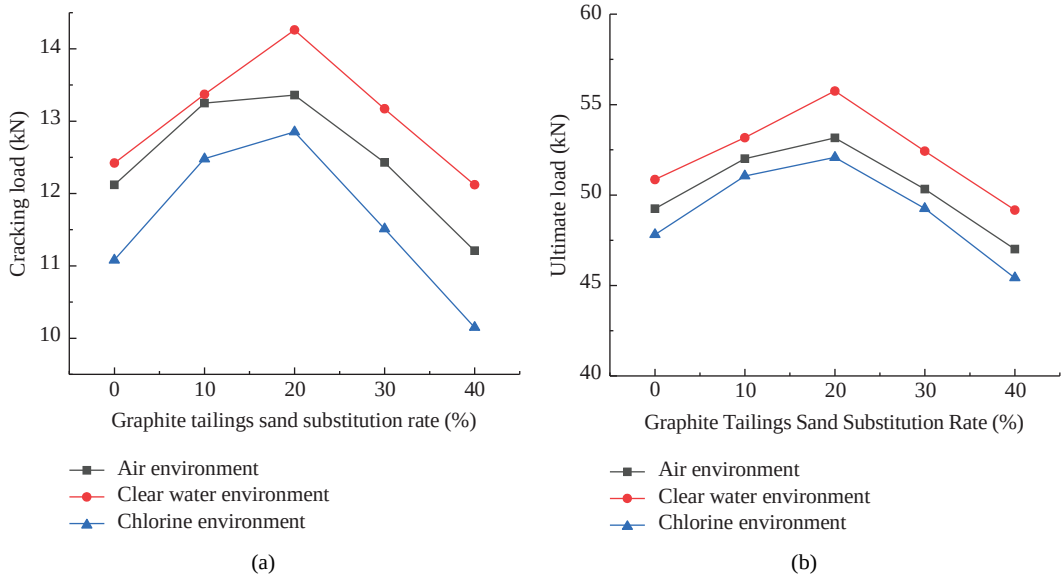

Figure 5: Influence of graphite tailing sand replacement rate on cracking load and ultimate load of test beam. (a) Cracking load and (b) Ultimate load.

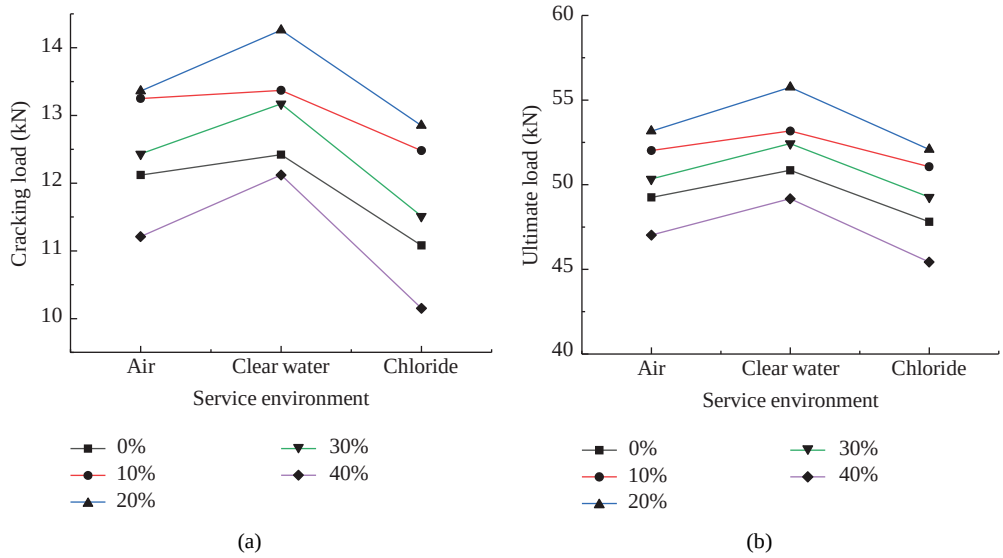

Figure 6: Influence of service environment on cracking load and ultimate load of test beam. (a) Cracking load and (b) Ultimate load.

beam is small. It can be seen from Figure 7(c) that after chlorine salt erosion of graphite tailings concrete beams, when the replacement rates of graphite tailings are 10% and 20%, the mid-span deflection growth rate of the test beam is slower than that of the ordinary concrete beam. When the replacement rate of graphite tailings is 40%, the mid-span deflection growth of the test beam is faster than that of the ordinary concrete beam, indicating that a small amount of graphite tailings can improve the flexural performance of reinforced concrete beams after chlorine salt erosion. It can be seen from Figure 7(d) that under the same load, the mid-span deflection of the graphite tailings concrete beam presents the law of clear water < air < chlorine salt.

The Variation of Mid-Span Concrete Strain. The mid-span concrete strain curves of concrete beams with diferent graphite tailings content under diferent loads in clear water and chlorine salt environment are shown in Figures 8 and 9. It can be seen from Figures 8 and 9 that with the increase of load, the concrete strain of each test beam shows an increasing trend. When the load is 20 kN, the concrete strain of the test beam CE-10 is larger than that of the FE-10, indicating that the resistance to deformation of the graphite tailings concrete beam decreases after being corroded by chloride. Under the environment of clear water and chloride salt, when the test beam was subjected to the same load, the cross-

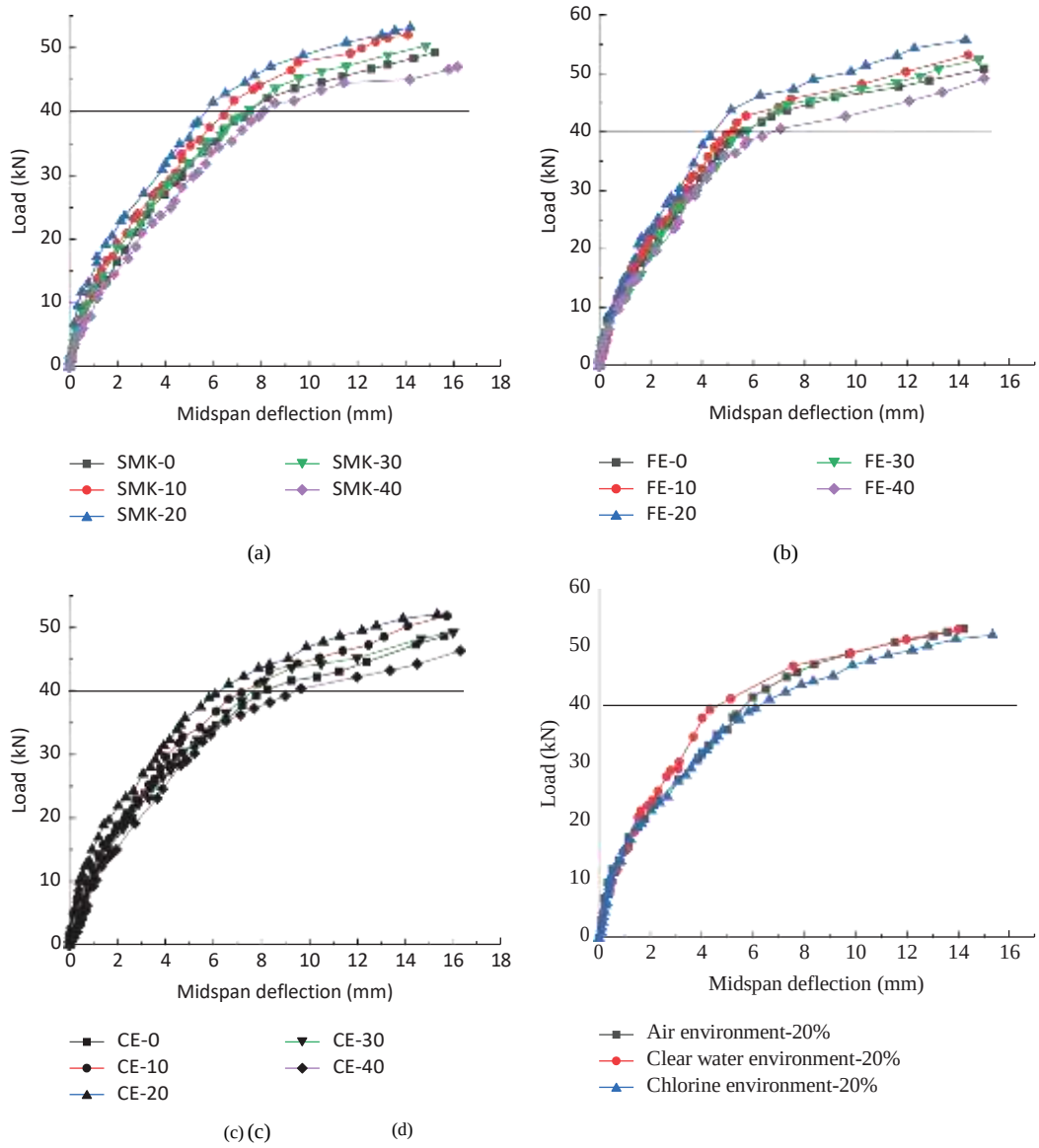

Figure 7: Load-deflection curve. (a) Air environment; (b) fresh water environment; (c) chloride environment; and (d) the replacement rate of graphite tailings is 20%.

sectional strain of concrete beams with diferent graphite tailings content was not significantly diferent, and the strain of concrete beams with 40% graphite tailings content was slightly higher. However, regardless of the amount of graphite tailings, the strain at each measuring point on the normal section is proportional to the distance from the point to the neutral axis, and the concrete strain of each measuring point on the mid-span section is linearly distributed. Therefore, in a clear water and chloride environment, the graphite tailings concrete beam still conforms to the plane section assumption. The test results show that the cross section of a graphite tailings concrete beam conforms to the plane section assumption under the three test environments listed above, which provides the experimental basis for the theoretical calculation of bearing capacity.

Longitudinal Steel Strain in the Mid-Span. The variation trend of the longitudinal tensile reinforcement strain in the mid-span of the test beam under diferent environments with the increase of load is shown in Figure 10. The load-steel strain curve of graphite tailings concrete beam can be divided into three parts: (1) In the early stage of loading, the test beam has not yet cracked elastic stage. In this stage, the tensile force is borne by concrete and steel, and the strain value of steel increases slowly and linearly. (2) From the cracking stage of the test beam to the yield stage of the steel bar, the tensile force of the test beam after cracking is transferred to the steel bar. In this stage, the steel bar strain is still linearly increased, but the growth rate is faster than that before cracking, and the slope of the steel bar strain-load curve is reduced. (3) When the steel bar yields to the failure stage, the load increases slightly and the strain increases sharply.

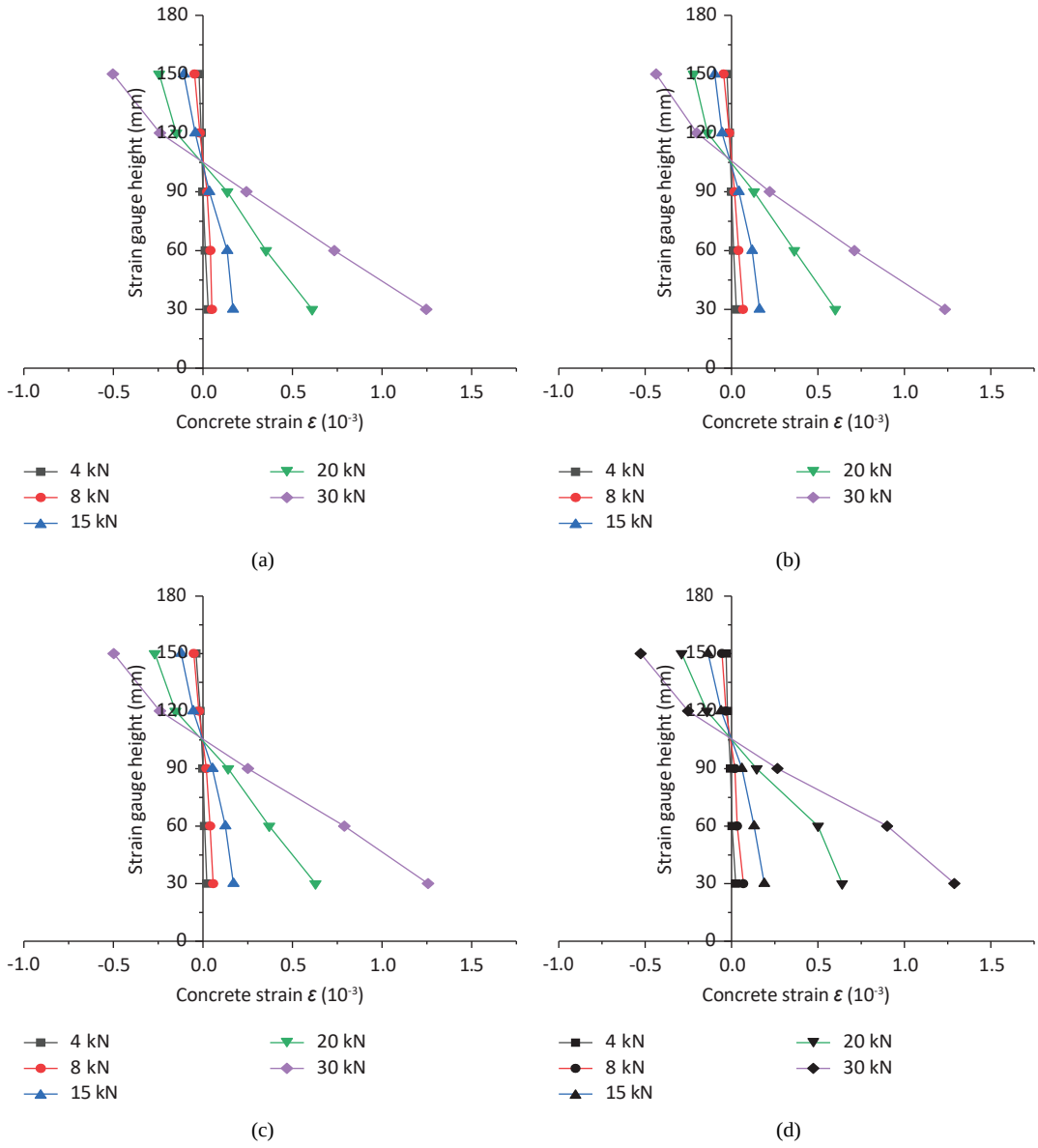

Figure 8: Strain distribution of diferent section heights in the middle of the test beam in a freshwater environment. (a) FE-10; (b) FE-20; (c) FE-30; and (d) FE-40.

It can be seen from Figure 10 that after water and chloride erosion, the longitudinal tensile steel strain of concrete beams with diferent graphite tailings replacement rates is consistent with that of ordinary concrete beams, and the slope of the curve is the same, indicating that the graphite tailings replacement rate has an insignificant efect on the steel strain. In the chloride environment, when each test beam bears the same load, the strain of the steel bar of the graphite tailings concrete beam with the replacement rate of 20% is smaller than that of the ordinary concrete beam and is smaller than that of the other graphite tailings replacement rate test beams. The reason is that when the replacement rate of graphite tailings is 20%, the porosity of the test beam is the smallest and the densest, and the influence of chloride ions into the concrete on the steel bar is the smallest, so the steel bar strain is small. This shows that the pore structure of concrete beams with graphite tailings is better than that of ordinary concrete beams with a small amount of graphite tailings, which is more conducive to the resistance of concrete beams to chloride corrosion damage.

Taking the replacement rate of graphite tailing sand of 20% as an example, the strain-load curve of the mid-span longitudinal tensile steel bar of 20% graphite tailing concrete beam in clear water and chloride environment is drawn, as shown in Figure 11. It can be seen from the diagram that chloride salt erosion has a slight efect on the strain of steel bars of graphite tailings concrete beams, but due to the short immersion time and low corrosion degree, chloride salt erosion has no significant efect on steel bars.

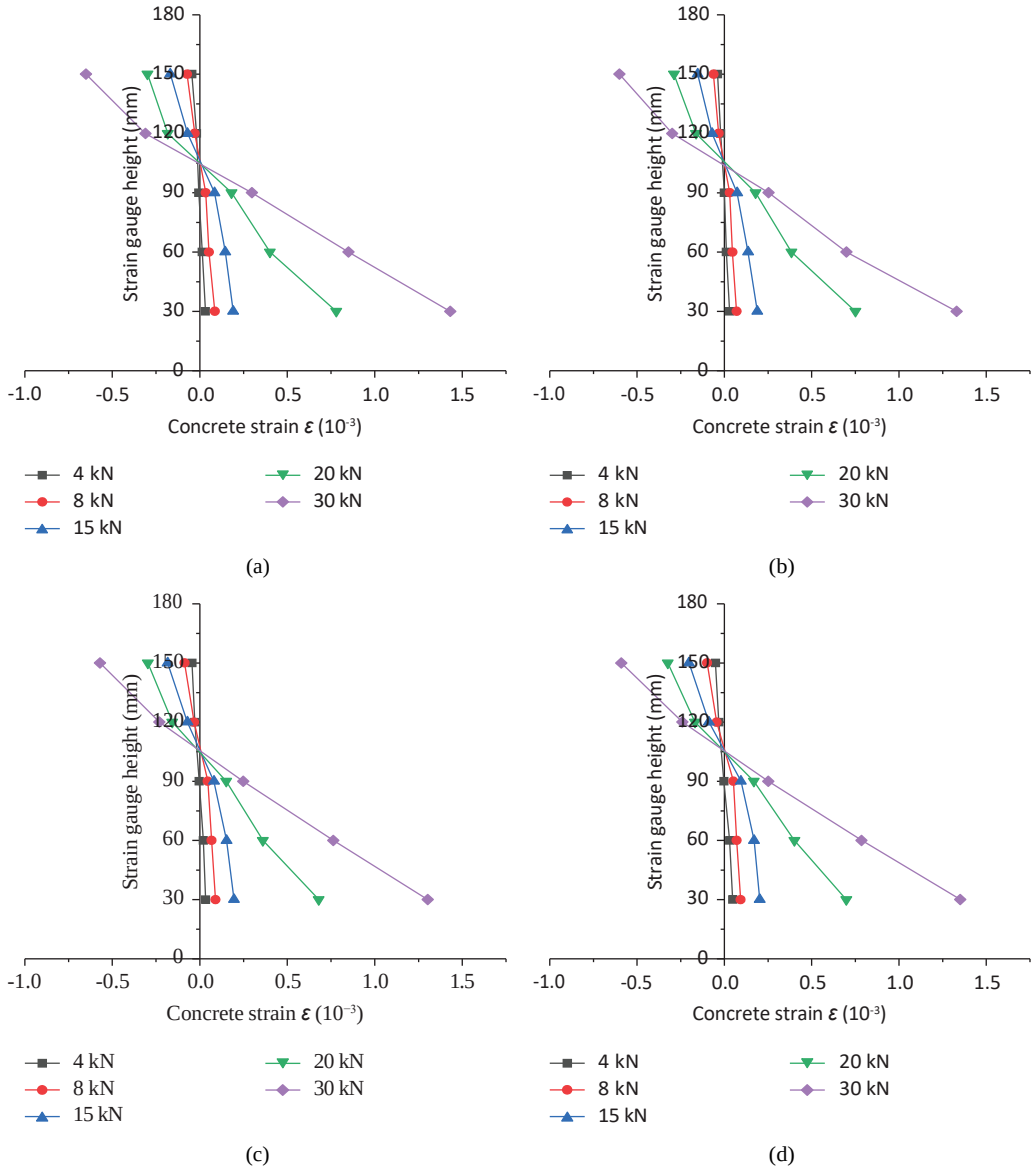

Figure 9: Strain distribution of diferent section heights in the middle of test beam in a chlorine environment. (a) CE-10; (b) CE-20; (c) CE-30; and (d) CE-40.

4. Analysis of Bearing Capacity of Graphite Tailings Concrete Beam Normal Section Under Chloride Erosion Environment

After chlorine salt erosion, the internal damage of graphite tailings concrete makes the strength of graphite tailings concrete decrease. The degradation of concrete's mechanical properties is the main factor afecting the bending performance of graphite tailings-reinforced concrete beams under the salt erosion environment. Therefore, in this section, the formula for calculating the ultimate bearing capacity of test beams after chlorine salt erosion is derived, and the influence of concrete strength changes with diferent graphite tailings contents on the bending bearing capacity of reinforced concrete beams after salt erosion is emphatically discussed. The theoretical value of the ultimate bearing capacity of the graphite tailings concrete beam after chloride corrosion is calculated by using the bearing capacity calculation formulas (1) and (2) of the normal section of the reinforced concrete beam [34]. The calculation results are shown in Table 4. In the table, M_c^y represents the ultimate bending moment test value of the graphite tailings concrete beam after salt corrosion, and M_u^y represents the theoretical calculation value of the ultimate bending moment of the graphite tailings concrete beam after salt corrosion.

$$M_u = \alpha_1 f_c b h_0 \left(1 - \frac{x}{2}\right) \quad (1)$$

$$\alpha_1 f_c b x = f_y A_s, \quad (2)$$

where, α_1 is the simplified stress figure coefficient of the concrete in the compression zone, taking 1.0; f_c is the measured compressive strength of graphite tailings concrete

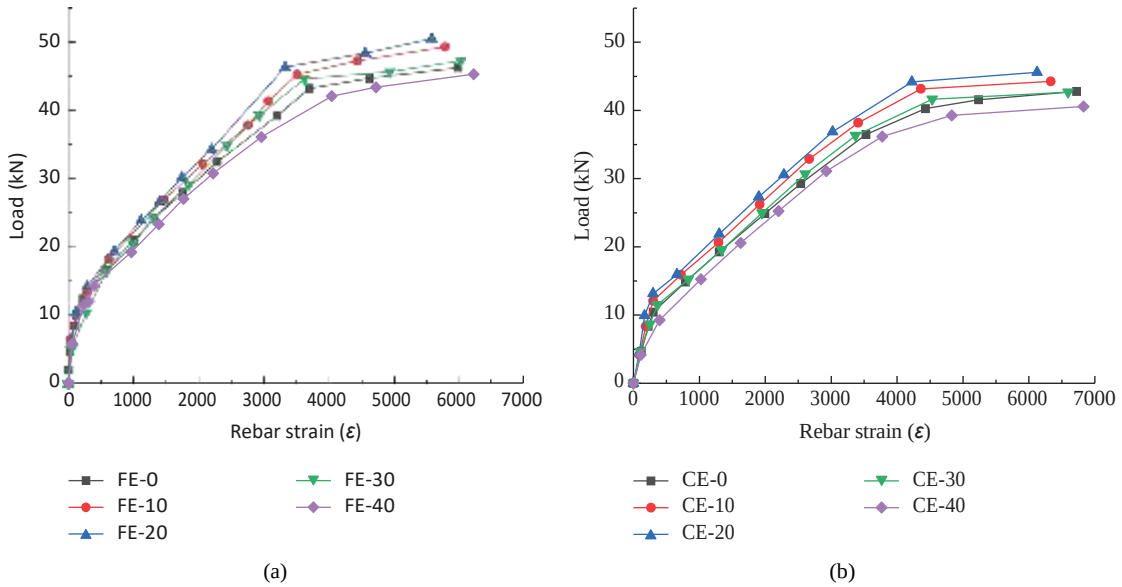

Figure 10: Strain-load curve of the longitudinal tensile steel bar in the middle of each test beam. (a) Fresh water environment and (b) chloride environment.

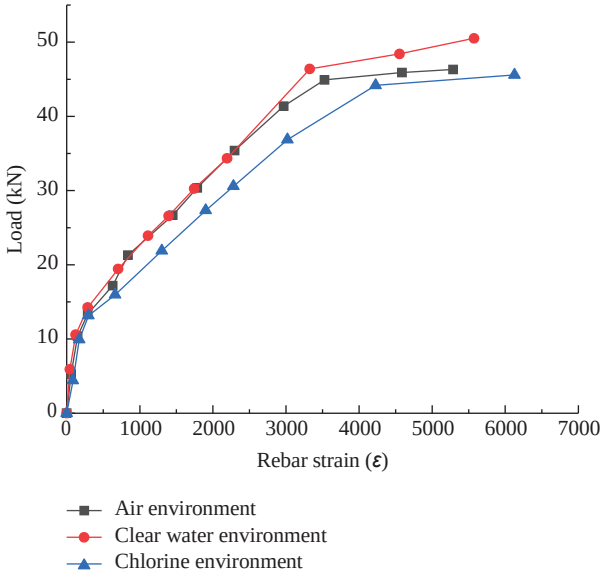

Figure 11: Strain-load curves of 20% graphite tailings concrete beams in diferent environments.

after chloride erosion, and takes the measured value, MPa; b is the beam width, mm; x is the height of the compression zone of the section, mm; h_0 is the efective height of the section, mm; f_y is the yield strength of longitudinal bars, and takes the measured value, MPa; and A_s is the efective cross-sectional area of the longitudinal reinforcement under tension, mm^2. The table is the comparison of calculated and experimental values of ultimate bearing capacity of graphite tailings concrete beams after chloride salt erosion.

From Table 4, the experimental values of graphite tailings concrete beams and ordinary concrete beams after chlorine salt erosion are greater than the calculated values, indicating that the ultimate bearing capacity of graphite

Table 4: Comparison of experimental and computational results according to formulas (1) and (2).

Specimen number	f_c (MPa)	M_c^y (MPa)	M_u^y (MPa)	M_c^y/M_u^y
CE-0	35.2	11.95	9.206	1.298
CE-10	36.1	12.76	9.218	1.384
CE-20	36.9	13.02	9.229	1.411
CE-30	35.1	12.32	9.204	1.339
CE-40	34.6	11.36	9.197	1.235

tailings concrete beams after chlorine salt erosion is feasible to calculate according to concrete specifications. To obtain the ultimate bearing capacity of concrete beams with different replacement rates of graphite tailings after chlorine salt erosion more accurately, two diferent fitting functions are used, and the correction coefficient of graphite tailings replacement rate is introduced. The data of concrete beams with diferent replacement rates of graphite tailings after chlorine salt erosion are numerically fitted.

Polynomial Fitting. To express the ultimate bearing capacity of graphite tailings concrete beams more accurately, the test results in Table 4 are fitted by polynomial function, and the fitting formula (3) and the fitting curve in Figure 12 are obtained. According to the fitting curve, the correlation coefficient of the fitting curve is 0.9879.

$$M^y = yM_u^y = Ax^2 + Bx + CM^y, \quad (3)$$

where x is the replacement rate of graphite tailings sand, (%); y is the correction factor; M_u^y is the theoretical calculation value of the ultimate bearing capacity of the test beam after chloride corrosion, MPa; and M^y is the corrected ultimate bearing capacity of the test beam after chloride corrosion, MPa; $A = -3.42143E-4$, $B = 0.01198$, $C = 1.29917$. Table 5 is

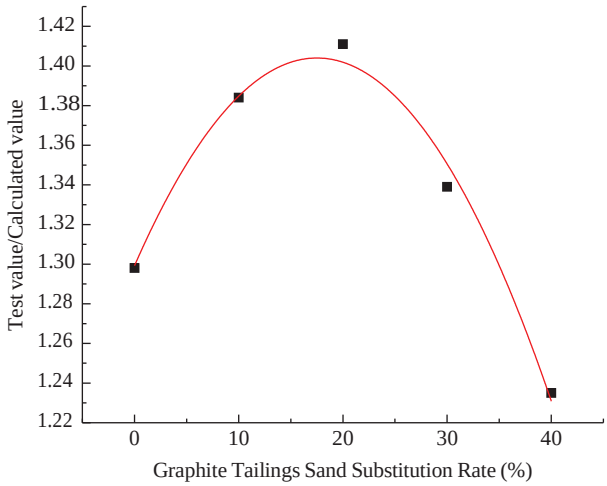

Figure 12: Polynomial fitting curve of ultimate bearing capacity of concrete beams with diferent replacement rates of graphite tailings after chloride erosion.

Table 5: Comparison of experimental and computational results according to formula (3).

The number of specimens	M^y (MPa)	M_c^y (MPa)	M_c^y/M^y
CE-0	12.02	11.95	0.9942
CE-10	12.82	12.76	0.9953
CE-20	13.00	13.02	1.0015
CE-30	12.50	12.32	0.9856
CE-40	11.40	11.36	0.9965

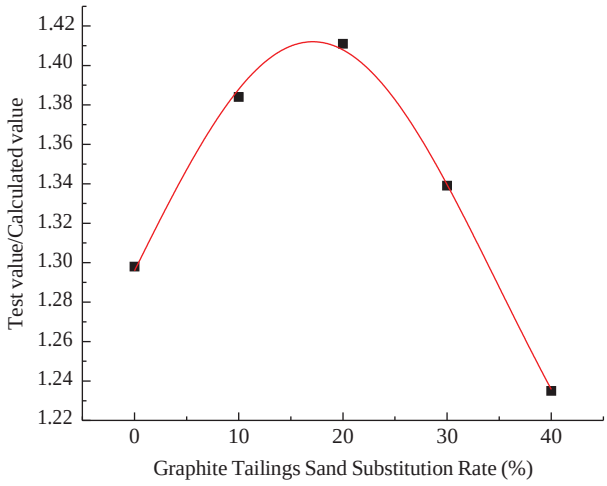

Figure 13: Gaussian function fitting curve of ultimate bearing capacity of concrete beams with diferent replacement rates of graphite tailings after chloride erosion.

a comparison of calculated and experimental values from formula (3).

Gaussian Function Fitting. The Gauss function fitting curve is shown in Figure 13. According to the fitting curve, the formula for calculating the ultimate bearing capacity of a normal section of graphite tailings concrete beam after chloride salt erosion is (4) and (5), and the correlation coefficient of the fitting curve is 0.9985. Compared with the polynomial fitting curve, the correlation coefficient of the Gaussian function fitting curve is closer to one, and the degree of coincidence is higher, indicating that the calculation formula of ultimate bearing capacity modified by the Gaussian function is more suitable for the calculation of ultimate bearing capacity of graphite tailings concrete beams after chlorine salt erosion. The axial compressive strength in the calculation formula needs to use the measured compressive strength value of graphite tailings concrete block after chlorine salt erosion. In practical engineering application, the compressive strength can be determined according to the empirical data or through experiments. At the same time, the modified formula can estimate the ultimate bearing capacity of the graphite tailings concrete beams with other mass replacement rates after chloride attack.

Table 6: Comparison of experimental and computational results according to formula (4).

The number of specimens	M^y (MPa)	M_c^y (MPa)	M^y/M_c^y
CE-0	11.93	11.95	1.0017
CE-10	12.78	12.76	1.0016
CE-20	12.96	13.02	1.0046
CE-30	12.33	12.32	0.9992
CE-40	11.38	11.36	0.9984

$$M^y = yM_u^y \tag{4}$$

$$y = y_0 + \frac{A}{w\sqrt{\pi/2}} \exp\left(-2\left(\frac{x - w_0}{w}\right)^2\right), \tag{5}$$

where M^y is the corrected ultimate bearing capacity of the test beam after chloride corrosion, MPa; y is the correction factor; M_u^y is the theoretical calculation value of the ultimate bearing capacity of the test beam after chloride corrosion, MPa; and x is the replacement rate of graphite tailings sand, (%); y_0 = 1.10078; A = 13.81231; w = 35.40572; w_0 = 17.10824. Table 6 is a comparison of calculated and experimental values from formula (4).

5. Conclusion

Graphite tailings are solid waste produced in the process of graphite mining, which has caused great damage to the natural ecological environment. Partial replacement of graphite tailings with construction sand is one of the effective ways to reuse solid waste. This paper studies the crack propagation law and bearing capacity of graphite tailings concrete beams under load. The following conclusions can be drawn from this study:

(1) Through experiments, it is found that the failure process and crack development process of graphite tailings concrete beams under three curing environments are the same, but the failure load of graphite tailings concrete beams under a chloride curing environment is small.

(2) In the three kinds of concrete curing environment, the fracture load and ultimate load of concrete beams with graphite tailings sand replacement rate of 20% are the largest. When the replacement rate of graphite tailings sand is the same, the fracture load and ultimate load of concrete beams under a chloride curing environment are the smallest.

(3) In three kinds of concrete experimental environment, when the concrete test beam under the same load, with the increase of graphite tailings replacement rate, the mid-span deflection of concrete beam decreases first and then increases. When the replacement rate of graphite tailings sand is 20%, the mid-span deflection of the test beam is the smallest; when the replacement rate of graphite tailings sand is 10% and 20%, the growth rate of the mid-span deflection of the test beam is slower than that of the ordinary concrete beam.

(4) Under the same load, the mid-span deflection of a graphite tailings sand concrete beam under the water experimental environment < the mid-span deflection of the graphite tailings sand concrete beam under the air experimental environment < the mid-span deflection of a graphite tailings sand concrete beam under the chloride experimental environment.

(5) The test results show that the cross section of a graphite tailings concrete beam conforms to the plane section assumption under the above three test environments, which provides the experimental basis for the theoretical calculation of bearing capacity.

(6) The experimental results show that the replacement rate of graphite tailings sand has negligible efect on the strain of steel bar. Comparing the strain values of the steel bars, it is found that the strain value of the steel bars in the graphite tailings sand concrete beam changes little than in the clear water experimental environment. In the chloride salt experimental environment, due to concrete and steel by chloride ion erosion, steel strain value changes large.

(7) Through the data fitting of the bearing capacity test results of graphite tailings concrete beams, the modified Gauss bearing capacity calculation formula is obtained. This conclusion has great reference value for the study of mechanical properties of concrete beams under chloride environment.

Data Availability

The data used to support the findings of this study are included within the article.

Disclosure

The manuscript was already published as a preprint based on the link https://papers.ssrn.com/sol3/papers.cfm?abstract_id﷿4033145.

Conflicts of Interest

The authors declare that they have no conflicts of interest.

References

[1] L. En-Ping, “Analysis on the development of Ofshore cities under the new development Pattern of double Circulation[J],” *Enterprise Economy*, vol. 40, no. 11, pp. 5–14+2, 2021.

[2] X. Jian-Zhuang, J.-Y. Shen, and Q. Gao, “Current situation and innovative technology for recycling of engineering waste soil[J],” *Journal of architecture and civil engineering*, vol. 37, no. 04, pp. 1–13, 2020.

[3] S. Fang-Zhi and X.-J. Li, “Summary of energy-saving and emission-reduction of road engineering,” *Road Machinery & Construction Mechanization*, vol. 28, no. 11, pp. 30–35+45, 2011.

[4] X.-Fu Han, “Improving Industrial development environment and Adhering to low Carbon green road-Thoughts on the present situation and development trend of concrete Industry in China,” *China Concrete*, vol. 4, pp. 42–46, 2011.

[5] H. Su, “Construction waste recycled concrete application,” *Building Technology Development*, vol. 36, no. 11, pp. 19-20, 2009.

[6] P. N. Hiremath and S. C. Yaragal, “Efect of diferent curing regimes and durations on early strength development of reactive powder concrete,” *Construction and Building Materials*, vol. 154, pp. 72–87, 2017.

[7] A. A. Mokhtar, R. Belarbi, and F. B. Jema, “Experimental investigation of the variability of concrete durability properties [J],” *Cement and Concrete Research*, vol. 1, no. 25, pp. 21–36, 2013.

[8] Y. Guo, Z. Chen, and X. Qin, “Evolution mechanism of microscopic pores in pavement concrete under multi-field coupling,” *Construction and Building Materials*, vol. 173, pp. 381–393, 2018.

[9] C. Zhang, L. Ben, Y. Yu, and Y.-J. Zhao, “Efect of graphite tailings on mechanical properties of recycled coarse aggregate concrete,” *Journal of Foshan University (Social Science Edition)*, vol. 39, no. 4, pp. 9–15, 2021.

[10] H. Liu, X.-F. Wang, and Z.-H. Yang, “Potential ecological Risk Assessment of Heavy Metals in Abandoned mining areas in Eastern Heilongjiang Province,” *Journal of Engineering*, vol. 9, no. 1, pp. 40–45, 2018.

[11] J. Thomas, N. N. Thaickavil, and P. M. Wilson, “Strength and durability of concrete containing recycled concrete aggregates,” *Journal of Building Engineering*, vol. 19, pp. 349–365, 2018.

[12] J. De Brito, J. Ferreira, J. Pacheco, D. Soares, and M. Guerreiro, “Structural, material, mechanical and durability properties and behaviour of recycled aggregates concrete,” *Journal of Building Engineering*, vol. 6, pp. 1–16, 2016.

[13] S.-Y. Wang, T.-H. Jiang, and X.-C. Zhang, "Study on chloride icon penetration resistance of high-performance concrete under double deterioration mechanism," *Transportation Science & Technology*, vol. 5, pp. 149–152, 2021.
[14] W.-M. Qian, J. Su, L. I. Yang, J. I. Wei, and J.-Y. Zhao, "Efect of ultra-low temperature and chloride on carbonation performance of ultra-high toughness cement-based composite," *Acta Materiae Compositae Sinica*, 2022.
[15] D.-X. Cai, B. I. Wen-Yan, and X.-M. Guan, "Simulation and experiments of the efect of coarse aggregates on the difusion of chloride ions in concrete," *Journal of Building Materials*, 2022, https://kns.cnki.net/kcms/detail/31.1764.TU.20220902.1720.002.html.
[16] M. Qing, J. Chang, and B.-Y. Sun, "Research on sulfate corrosion resistance and Microstructure characteristics of Iron tailings concrete," *Multipurpose Utilization of Mineral Resources*, 2022, https://kns.cnki.net/kcms/detail/51.1251.td.20220831.1653.002.html.
[17] D. Shang-Qin, *Experimental study on Mechanical Properties of sea sand concrete Beams in marine Environment*, Guangxi University, Guangxi, China, 2020.
[18] S.-P. Yin, Y. Yu-Lin, and N. Ming-Wang, "Bending performance analysis of TRC reinforced beams under chloride erosion[J]," *Journal of Huazhong University of Science and Technology (Natural Science Edition)*, vol. 47, no. 02, pp. 7–13, 2019.
[19] S. Qing-Bo, J.-J. Zhang, and F.-N. Zhou, "Experimental study on chloride ion erosion of Joints in concrete Bridge[J]," *Railway Construction Technology*, vol. 8, pp. 30–34+110, 2022.
[20] X.-Y. Mou, Y.-W. Wang, and L. Shi-Bao, "Prediction of effective chloride difusion coefficient of recycled aggregate concrete based on multiscale analysis," *Acta Materiae Compositae Sinica*, 2022.
[21] Z.-G. Sun, L. Xiao-Kui, and L. Hong-Biao, "Flexural strengthening Efectiveness of chloride corrosion damaged RC beams by using PVA-ECC," *Journal of Basic Science and Engineering*, vol. 30, no. 04, pp. 963–973, 2022.
[22] H. Liu, Q. Zhang, V. Li, H. Su, and C. Gu, "Durability study on engineer cementitious composites (ECC) under sulfate and chloride environment," *Construction and Building Materials*, vol. 133, no. 15, pp. 171–181, 2017.
[23] M. Sahmaran, V. C. Li, and C. Andrade, "Corrosion resistance of steel-reinforced engineer cementitious composite beams," *ACI Materials Journal*, vol. 105, no. 3, pp. 243–250, 2008.
[24] Y. Zhang, N. Ueda, H. Nakamura, M. Kunieda, and H. Nakamura, "Behavior investigation of reinforced concrete members with flexural strengthening using strain-hardening cementitious composite," *ACI Structural Journal*, vol. 114, no. 2, pp. 417–426, 2017.
[25] A. S. Shanour, M. Said, A. I. Arafa, A. Maher, and A. I. Arafa, "Flexural performance of concrete beams containing engineered cementitious composites," *Construction and Building Materials*, vol. 180, no. 20, pp. 23–34, 2018.
[26] L. Hong-Bo, Yu-X. Zhang, and Z.-R. Wang, "Research on compressive strength and impermeability of graphite tailings cement mortar [J]," *Engineering Journal of Heilongjiang University*, vol. 10, no. 04, pp. 16–20, 2019.
[27] H. Liu, B. Li, J. Xue, J. Hu, and J. Zhang, "Mechanical and Electroconductivity properties of graphite tailings concrete," *Advances in Materials Science and Engineering*, vol. 2020, Article ID 9385097, 20 pages, 2020.
[28] Z.-R. Wang, B. Li, and L. Hong-Bo, "Degradation characteristics of graphite tailings cement mortar subjected to freeze-thaw cycles," *Construction and Building Materials*, vol. 234, pp. 132-133, 2020.
[29] L. Hong-bo, D.-S. Zhang, and L. Xiao-li, "Research on the Compress-ion sensitivity of graphite tailings concrete," *Journal of Engineering of Heilongjiang University*, vol. 6, no. 01, pp. 22–27, 2015.
[30] S. Xiao-wei, W.-qi. Zhang, and Qi. Wang, "Research on the performance of graphite tailings foamed concrete," *Nonmetallic Minerals*, vol. 43, no. 03, pp. 9–13, 2020.
[31] W.-X. Sun, *Study on Durability of Graphite Tailings Concrete*, Heilongjiang-ang University, Heilongjiang, China, 2019.
[32] F. Bo-Ya, X. Xia, Z. Zhu, and X. Zhu, "Experimental study on flexural behaviour of graphite tailings concrete beam in chloride environment," 2022, https://papers.ssrn.com/sol3/papers.cfm?abstract_id=4033145.
[33] National Standard of the People's Republic of China, *GB/T 50152-2012 Standard for Test Methods of concrete structure*, China Architecture & Building Press, Beijing, 2012.
[34] National Standard of the People's Republic of China, *GB 50010-2010 Code for Design of concrete structures*, China Architecture & Building Press, Beijing, 2010.